Parametric Analysis of Small Scale Cavity Receiver with Optimum Shape for Solar Powered Closed Brayton Cycle Applications

Daabo, Ahmed M.; Ahmad, Abdalqader; Mahmoud, Saad; Al-dadah, Raya K.

DOI:
10.1016/j.applthermaleng.2017.03.093

Document Version
Peer reviewed version

Citation for published version (Harvard):
Daabo, AM, Ahmad, A, Mahmoud, S & Al-dadah, RK 2017, 'Parametric Analysis of Small Scale Cavity Receiver with Optimum Shape for Solar Powered Closed Brayton Cycle Applications', *Applied Thermal Engineering*. https://doi.org/10.1016/j.applthermaleng.2017.03.093

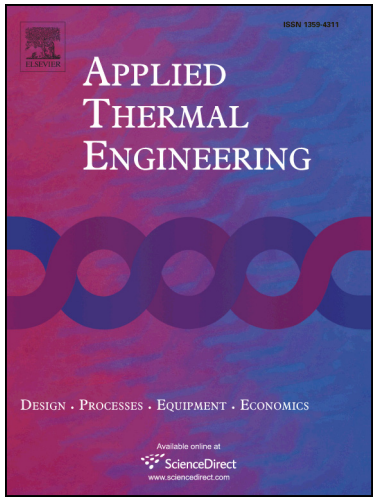

Parametric Analysis of Small Scale Cavity Receiver with Optimum Shape for Solar Powered Closed Brayton Cycle Applications

Ahmed M. Daabo, Abdalqader Ahmad, Saad Mahmoud, Raya K. Al-Dadah

PII: S1359-4311(17)31868-9
DOI: http://dx.doi.org/10.1016/j.applthermaleng.2017.03.093
Reference: ATE 10097

To appear in: *Applied Thermal Engineering*

Received Date: 11 August 2016
Revised Date: 21 February 2017
Accepted Date: 20 March 2017

Please cite this article as: A.M. Daabo, A. Ahmad, S. Mahmoud, R.K. Al-Dadah, Parametric Analysis of Small Scale Cavity Receiver with Optimum Shape for Solar Powered Closed Brayton Cycle Applications, *Applied Thermal Engineering* (2017), doi: http://dx.doi.org/10.1016/j.applthermaleng.2017.03.093

Parametric Analysis of Small Scale Cavity Receiver with Optimum Shape for Solar Powered Closed Brayton Cycle Applications

Ahmed M. Daabo[a,b]*, Abdalqader Ahmad[a], Saad Mahmoud[a], Raya K. Al-Dadah[a]
[a] The University of Birmingham, School of Engineering,
Edgbaston, Birmingham, B15-2TT, UK
*Email: axd434@bham.ac.uk, ahmeddaboo@yahoo.com
[b] The University of Mosul, Mechanical Engineering Department, Ninawa, Iraq

Abstract

Day after day the interest in the renewable clean energy is increasing because of the enormous advantages that it has. One of the main forms for the renewable energy is the solar which has been used through power systems such as the Concentrated Solar Power (CSP), which shows a remarkable enhancement recently. The current study examines different arrangements of an open cavity receivers with an aperture area of 0.02835 m^2 and an average flux values ranged from 2.5 to 15 kW/m^2. By employing an advanced ray tracing OptisWorks software, which uses the Monte-Carlo ray-tracing technique for predicting the flux distributions, to decrease the optical losses and computational fluid dynamic CFD analysis to minimize the thermal losses, the fluid exit temperature can be maximised. The exact values and distribution of the received irradiance by the surface area of each helical coil, inside the receiver shape, was subsequently transferred and used as an input parameter using the User Defined Function, UDF, in order to numerically simulate the fluid flow and calculate the amount of heat transfer to the working fluid through the CFD analysis. Different scenarios including each, the shape configuration, the reflector diameter, and the helical coil pitch has been intensively carried out in the study. Results showed that compared to 0.5D pitch value, the zero pitch showed better performance in both optically and thermally. Moreover, an enhancement up to around 7% in the overall thermal performance was achieved when the receiver aperture area was covered by glass. Finally, some analysis for closed Brayton cycle was considered and the results showed the 80% overall system efficiency is applicable if there is more than one application is integrated in the system.

Keywords: Thermal Receiver, Pitch Effect, Ray-Tracing, CFD Analysis, Closed Brayton Cycles.

1. Introduction

There is no doubt that the energy demand is continuously increasing with increasing the world population which leads to more and more call for fossil fuel consumption and the problems of CO2 emission will be raised. Some solution, however, such as the solar energy might help and save the environment from this threat if both researchers and the responsible people pay more attention to this important topic. While there are some interest in some fields of the solar energy especially the photovoltaic cells, some other important application like the Concentrated Solar Power (CSP) is still have a lot to be analysed. The main function of this application is gathering the power coming from

the sun, using different types of Concentrating Solar Collector, and directing it inside a thermal cavity receiver to change the solar radiation to a thermal energy. In CSP cycles for example Brayton, Rankine, and Stirling cycles the thermal receiver has the main role in transferring the received heat to the working fluid in order to power one of these thermal cycles. Brayton Cycle has the ability to be a promising technology compared to other cycles because of the advantages, besides using the air as a working fluid, such as the high efficiency, the low pressure drops and cost [1, 2]. Improving performance thermal system of the cycle, including the parabolic reflector and the thermal receiver, has been studied by different researchers. For example a cavity receiver, for saturated water/steam, with various depths was numerically analysed to know their effect on the thermal efficiency was considered by Tu et al [3]. The results showed that there is a relation between the receiver thermal efficiency and each, the heat flux distributions and the wall temperature and the highest value were found when the receiver is stretched. The influence of various receiver shapes and positions on the uniformity of each; the flux and temperature inside the receiver, for Stirling engine indoor tests, application was numerically studied by Zhigang et al [4]. On the other hand the investigating a parabolic dish collector coupled with a cavity receiver for Organic Rankine Cycle (ORC) application was recently achieved by Loni et al [5]. In their study the researchers studied the effect of each the cavity depth and the tube diameter at different inlet temperature and mass flow rate values on the overall performance of the thermal receiver and they found that the lower inlet fluid temperature and smallest tube diameter will lead to higher overall thermal efficiency for the thermal part of the system. The relationship between the cavity receiver configuration and the optimum location of its focal point for three different shapes or thermal receiver was deeply studied by Daabo et al [6]. In their study the authors found that for each specific cavity configuration there is a specific optimum location for the focal point which gives the best flux distribution. Interestingly, they have also found that the location of those configurations is also influenced by the optical properties of the receivers' internal surfaces. Furthermore, the thermal evaluation for the same receivers' shapes by analyzing the effect of the opening ratio on the amount of heat losses for Brayton cycle application was also achieved by the same authors [7]. Milind et al [8] experimentally used a hemispherical shape receiver with water as a working fluid, in order to estimate the natural convection heat loss for a 0.54 m cavity diameter and for different inclination from 0^o to 90^o. They found that the minimum heat convection loses was noticed to be at 90o and the maximum one was at 0^o. The influence of wind speed on the amount of heat losses through a completely open cylindrical receiver shape, electrically heated at stable heat flux, was experimentally studied by Shuang et al [9]. Beside the correlations that the authors have conducted, they showed that the amount of combined convection heat loss is proportionally affected by the wind speed, while the opposite was the case for both radiation and conduction heat losses. Moreover, for forced convection, the value of the heat loss showed less influence to the inclination of cavity receiver in contrast to that of no-wind conditions. Other studies such as [10, 11, 12 and 13] thermally evaluated the overall performance of the small scale cavity receiver at various receiver

inclinations and they found the inclination of 90^{o} gives the lowest overall heat losses. The overall evaluation, optically and thermally, of three different cavity receiver shapes, cylindrical, conical and spherical, for the small scale Brayton cycle application was achieved by Daabo at al [14] using three dimensional numerical analyses. In their study the authors investigated different factors such as the cavity shape, the absorptivity and they found that the conical shape behave better than the other two shapes, cylindrical and spherical. In recent times, quite a few attempts [15- 18] by various researchers for different applications have been achieved to optimize the geometry of receiver, by investigating different geometrical parameters, with the aim of enhancing the overall performance of the system. The relationships between the maximum allowable flux density that hits the internal surface of receiver and its wall's diameter, thickness and the velocity of the working fluid was studied by Liao et al. [19]. The results indicated that the density of the allowable irradiance can be improved if higher yield strain for the tube material used or with increasing the velocity of the Heat Transfer Fluid (HTF) or even by decreasing the thermal resistance, wall thickness and diameter of the tube. M. Prakash studied numerically the natural convection heat loss with three different diameters of cylindrical solar cavity receiver contains a helical coil and air as a working fluid. The study considered different inclinations with different inlet temperature values and tow values of opening ratio, 1 and 0.5, using the Fluent CFD [20]. In his study a new correlation included Nusselt number, Rayleigh number, the receiver inclination, and opening ratio was proposed. Wang et al [21] studied the impact of different factors like the rim angle, the aperture size and the inlet/outlet arrangement of the solar thermal receiver of the parabolic reflector on the temperature distributions of the receiver wall for argon as a working fluid. The results showed when aperture area of the receiver reduces to the half, each; the averages of argon and wall temperatures inside the receiver augmented by 9.2% and 7.5%, respectively.

As it can be seen from the mentioned literature above, the study of variety scales is being interesting and tends to be the topic of the current and near future studies as it can contribute in enhancing a main part of the solar system, optically and thermally. So, following studies done in [7 and 14], in the current study some emphasis has been put to achieve the optimum shape for the conical shape receiver. Moreover, the optical and thermal effect of some other parameters such as reflector diameter, irradiance value, tube pitch, on the overall performance of closed Brayton cycle has been figured out using 3- D analysis. Some analysis regarding the chosen closed Brayton cycle have also been included in the present study. This cycle has been selected in order to evaluate the possibility of adding another application, which is the heating system, while keeping the advantages of Brayton cycle such is cleanliness and the working fluid availability.

2. The Methodology

In this study, the thermal system, parabolic dish reflector and thermal receiver, of closed Brayton cycle configuration figure (1) has been proposed for a domestic application. Following the studies done previously by the authors who showed that the conical shape experienced the highest optical efficiency, this study is focused on the conical shape with some results about the other two shapes. After, the effect of each; the receiver shape, and the pitch of its helical tube on the optical, thermal and overall system performance has intensively discussed using two different types of software. After the optical properties for each; the source, the parabolic reflector and the receiver specified, the numerical analysis, using OptisWorks® 2016, has been achieved and the amount of received flux by the aperture area and on the helical tube surface was determined.

At this point it is important to mention that a parametric study was carried out on the dimension of each receiver configuration with the aim of finding the optimum shape where the flux can successfully reach and cover all their internal surfaces. The real of flux and distribution was transferred, using the UDF, to be used as an input parameter during the thermal analysis which has been achieved, in order to specify the amount of overall heat losses and determine the value of outlet fluid temperature, using the CFD technique. Consequently the effect of the above mentioned parameters was also investigated and their influence on the cycle and system efficiency has also been figured out. The other important thing is that in this study the authors have only considered the 20 mm diameter tube because it is the lowest computational cost compared to the smaller dimeter values.

3. Heat Losses

The total heat losses, equations (1 and 2), are the ones considered in the thermal balance during the solution.

$$Q_T = Q_{Cond} + Q_{Conv} + Q_{Rad} \quad (1)$$

$$Q_T = mC_P(T_{fi} - T_{fo}) \quad (2)$$

Equations (3-5) can be used for calculating the conduction, convection and radiation, is characterised in respectively [22] and [23].

$$\frac{\partial^2 T}{\partial X^2} + \frac{\partial^2 T}{\partial Y^2} + \frac{\partial^2 T}{\partial Z^2} + \frac{g}{k} = \frac{1}{\sigma}\frac{\partial T}{\partial t} \quad (3)$$

$$Q_{Conv} = hA \quad \text{, where} \quad h = kNu/L \quad (4)$$

$$Q_{Rad} = \varepsilon\sigma(T_{Sur}^4 - T_{Amp}^4) \quad \text{, where} \quad (5)$$

ε is the surface emissivity and σ is the Boltzmann constant.

For cavity receivers' models, the recommended correlations some for calculating Nusselt numbers are defined in terms of receiver configuration and the applied boundary conditions. Among them, the ones presented in references [20], [24] and [25], equations (6 and 7), are thought to be the most familiar correlations for the thermal cavity receivers.

$$Nu_{D\,WI} = 0.0303 Gr_D^{0315}\left(1+\cos(\phi)\right)^{3.551}\left({T_\omega}/{T_\infty}\right)^{-0.086}\left(\frac{d_{ap}}{D_{Cav}}\right)^{0.878} \quad \text{for } 10^6 \le Gr \le 10^7 \tag{6}$$

$$Nu_D = 0.0133 Gr_D^{1/3}\left(1+\cos(\phi)\right)^{2.6}\left(\frac{d_{ap}}{D_{Cav}}\right)^{0.47} \tag{7}$$

Where d_{ap} is the aperture diameters and D_{Cav} is the cavity diameter

The radiative mode of heat losses can also be figured out analytically by determining each; the view factor, the radiosity and the emissivity of each receiver shape. So, the overall losses can be calculated by equations (8 and 9) [26-29].

$$Q_{Rad\,i} = \sum_{j=1}^{N} F_{i,j}\left(J_i - J_j\right) \tag{8}$$

$$Q_{Rad} = \varepsilon_{eff}\sigma A_{ap}\left(T_{wall}^4 - T_{amp}^4\right), \text{where } \varepsilon_{eff} = \frac{1}{\left(\frac{1-\varepsilon}{\varepsilon}\right)}\frac{A_{ap}}{A_w} \tag{9}$$

Where F and J are the view factor and the radiosity; and i and j represent any two faces inside the thermal cavity receiver.

4. Numerical Simulation

For the sake of accuracy, three-dimensional ray tracing analysis has been employed as a tracing technique of OptisWorks® 2016 in order to imitate the optical behaviour of various solar systems by using ray techniques. Recently this software has been extensively utilized by numerous researchers [30-34] because of its high reliability. Once the geometry of each receiver with its internal helical tube modelled using SOLIDWORKS® 2016, the assembly (source, parabolic reflector and thermal receiver) of each model was transferred and modelled using OptisWorks® 2016. The main purpose behind this step is to find the value of the incoming flux, absorbed flux and reflected flux at each on the helical tube surface and its cavity of each thermal receiver. The considered dimensions and specifications of the parabolic dish reflector and thermal receivers are presented in Table I and the relevant data regarding the helical tube inside each cavity receiver mentioned in Table II. After characterizing the optical properties of each; the parabolic reflector and the thermal receiver, to make

them reflect and received respectively the incoming rays which has come from the proposed source. Moreover, in order to precisely determine the position of the focal point, both the parabolic diameter and its rim angle need to be specified. Figure (2) displays the parabolic dish reflector together with one of the modelled receiver, the conical shape, all through the ray-tracing analysis.

5. Thermal Analysis and CFD Models

Once the calculations of the received flux on the helical tube surface and the receiver cavity completed, the geometry of each receiver can be transferred to the CFD analysis. The main aim of this step is to calculate the amount of solar energy that has been received by the HTF after extracting the heat lost to the surroundings which can be determined based on the principles of heat losses. At this point it is important to mention that all the three types, convection, conduction and radiation, have been together considered during the numerical calculation. In spite of the fact that the CFD technique is one of the most efficient approaches which have being utilizing recently to attain the required analysis for numerous applications, this technique will never be 100% reliable unless correctly considering some specific points during the CFD setting. For example, setting the accurate data through the boundary conditions with a lesser amount of imprecision or guessing will provide more precise results. Also, the exact mathematical model of the relevant problem needs to be carefully considered. The reliability of this technique is not fixed and instead, it depends on the problem circumstance [35] and [36] for example it is considered high for specific simulation conditions such as those of laminar flows, or in case of single phase flows which are the situation relevant to this study. Here it is significant to refer to the flow type which was turbulent and also to the chosen element and its size which are the tetrahedral type and smooth medium size [37]. By completing the required quality of mesh was obtained, which was around 850000 elements figures (3A, 3B), the model becomes ready to the following assumptions, which have been considered in the numerical analysis. More details will be found in the next section.

6. Thermodynamic Analysis of Closed Brayton Cycle

In order to evaluate the effect of both the optical and the thermal performances of each receiver configuration on the overall efficiency of the cycle in interest, Matlab code has been initiated at the conditions. As it was shown in figure (1) the working fluid enters the compressor at point 1 in order to increase its pressure before entering the thermal receiver where its heat will be raised. Here, it is important to mention that the amount of heat used in the Matlab code was determined after extracting the optical and the thermal losses by using the two types of mentioned software. After that it passes through a recuperator in order to take advantage of the heat which the leaving air, leaving from the turbine, has. The third component that the air enters is the thermal receiver which where most of the concentrated heat, from the parabolic dish reflector, is focused on its internal surface which has the helical tube. Next, the compresses and heated air is going to release its energy in the turbine where

this energy will be converted to a kinetic energy, rotation speed in the rotor part of the turbine and generate some power. The air which is leaving the turbine will enter the recuperator again in order to exploit its heat and the remaining heat will increase the temperature of cycling water in a small tank which can be suitable for domestic application.

The power required for compressor, W_C, can be calculated using equations 10 [38]:

$$W_C = \dot{m}(h_2 - h_2) \quad (10)$$

The heated compressed air exit from thermal receiver delivers the energy to the turbine in order to produce power which can be determined as shown in the following equation:

$$W_T = \dot{m}(h_4 - h_5) \quad (11)$$

The heat supplied to the system is coming from the solar thermal system, parabolic dish and receiver is:

$$Q_{Add} = \dot{m}(h_4 - h_3) \quad (12)$$

$$\text{Thermal Power} = \dot{m}(h_6 - h_1) \quad (13)$$

The extent to which a regenerator approaches an ideal regenerator is called the effectiveness, ε, and is defined as:

$$\varepsilon = \frac{h_3 - h_2}{h_5 - h_2} \quad (14)$$

The net work done which can be gotten from the cycle is given by:

$$W_{Net} = (W_T - W_C) \quad (15)$$

In order to extract some of its energy, the expanded air passes through the recuperator. So, the heat gained by the compressed air can be calculated using equation 16.

$$Q_G = \dot{m}(h_2 - h_3) \quad (16)$$

The other cycle is that which the compressed air will follow before it completes its cycle and enters the compressor again, is that when the remaining heat will be released in a cycling water to increase its temperature where this heated water can be used in any relevant application. By doing so, it can be granted that the compressed air will enter the compressor, in the next cycle, at low temperature which of course will affect well on the compressor efficiency.

To increase the overall cycle efficiency, the rejected heat is stored in a storage tank and can be used to heat water for domestic use and at the same time decreases the compressor inlet temperature. The amount of this energy can be determined using equation 18.

$$Q_{cRej} = \dot{m}(h_5 - h_2) \tag{17}$$

The thermal closed Brayton cycle efficiency is given by:

$$\eta_{th} = \frac{\mathrm{W_{Net}}}{\mathrm{Q_{Abs}}} \tag{18}$$

Similarly, the total efficiency of the all system, thermal and heating, can be determined using the following equation:

$$\eta_{Sys} = \frac{\mathrm{W_{Net}} + Thermal\ Power}{\mathrm{Q_{In}}} \tag{19}$$

7. Boundary Conditions

The most essential assumptions are shortened in the next following points:

1- The mass flow rate was fixed at 0.01 Kg/s for the Brayton cycle the working fluid of ideal gas for air was chosen as HTF. However, during the cycle analysis the amount of mass flow rate was not fixed as it is essential in the used code.

2- Moreover, steady state, no buoyancy (the gravitation effect) and surface to surface solution method were chosen and included during each run.

3- The inlet temperature was assumed to be 375 K, for the closed Brayton cycle, for all the running cases. The reason behind that is the temperature of the compressed air is supposed to be raised after passing the compressor.

4- The outlet condition regards the pressure is kept to be at atmospheric pressure and at the relevant suitable conditions with no wind influence was neglected by means of natural convection only will be the convective heat losses [39]. Moreover, the model of the receiver was maintained vertically, 90^{o} only, as this alignment attains the lowest amount of convective heat losses [25] and [40].

5- Both the internal surfaces of the cavity receiver, the outer surfaces of the helical tube and their real distribution of the irradiance flux is imported from the OptisWorks to the ANSYS with its Fluent solver for all the cases.

6- Moreover, the value of conductive heat losses were decreased as the external surfaces of the receivers' was covered by a high insulation material [39]. More details about the utilized materials can be found in table III.

7- Finally, the continuity, energy and Navier-Stokes momentum equations (20- 22) were simultaneously running in order to control the flow of each fluid in the helical tubes of each thermal

receiver.

For calculating the radiation losses each model needs the relevant value of view-factor [41] so this was also calculated before computing the radiation heat losses. The conditions for convergence for the residuals of both the velocity equation and the continuity equation were at the order of 10^{-5} and the energy equation was set to 10^{-7} in order to achieve more precise results. The solutions were achieved once the mentioned convergence conditions were met.

$$\frac{\partial \rho}{\partial t} + \frac{\partial}{\partial x_i}(\rho u_i) = 0 \tag{20}$$

$$\frac{\partial}{\partial t}(\rho u_i) + \frac{\partial}{\partial x_i}(\rho u_i u_j) = \frac{\partial}{\partial x_j}\left[-\rho\delta_{ij} + \mu\left(\frac{\partial u_i}{\partial x_j} + \frac{\partial u_i}{\partial x_i}\right)\right] + \rho g_i \tag{21}$$

$$\frac{\partial}{\partial t}(\rho C_P T) + \frac{\partial}{\partial x_i}(\rho u_i C_P T) - \frac{\partial}{\partial x_i}\left(\lambda \frac{\partial T}{\partial x_i}\right) = S_T \tag{22}$$

8. Optical and Thermal Validation

In order to confirm each the optical and the thermal procedure followed by the current work, some experimental results are extremely requested. So, for the optical one, some indoor experimental works were already completed by a colleague [42] who used an electrical source and the comparison between the simulated and the experimental results are shown in figure (4). By contrast, the procedure which was followed during the thermal work was validated by using some experimental works done by other researchers because the rig is on preparing at the moment. For the reason that references [43], [44] and [45] have relatively sufficient given data, those references have been selected and intensely examined with the purpose of validating the models of the current study and the results showed very good agreement. As shown in figure (5), the results of the current model and those which were chosen from the experimental studies were in very good agreement especially with the model proposed by reference [45]. Having said that, the present study has underestimated all values of heat loss at the investigated inclinations because of the interior air velocity in the cavity was presumed to be equal to zero but experimentally is not the case. The other reason might be relating to the irradiance on the external tube surfaces was assumed to be uniform; however, this is not the condition in experimental work. Moreover, the tube material was assumed as smooth and uniform which is not the case experimentally. Nevertheless, the current CFD results and the experimental, which were applied in the validation, have showed very good agreement at the inclination of 90^o, i.e. the cases of the current study where the thermal receiver was faced down.

9. Results and Discussions

In this research, the examined outcomes are built based on the value of gained irradiance, from the source, and the total value of heat losses from the investigated thermal receiver to its environments.

For the collected irradiance, it can be seen that the configuration of the thermal receiver has a major impact on the distribution irradiance on the helical surface inside the cavity of receiver. This in fact plays an important role in terms of the quantity of heat losses. An optical evaluation for the receiver using different configuration of the conical shape with different collector's diameter and irradiance values, was also taken into account in order to achieve the optimum conical shape for the receiver. The 3D simulation of the thermal receiver with its tube was done firstly using the OptisWorks 2016, in order to evaluate the optical performance and then transferred, by considering its real value and distribution, using UDF technique in ANSYS-CFD solver for assessing the thermal performance with and without a glass on the receiver's aperture. Consequently, the influence of each; the pitch and the flux uniformity on the amount of heat losses and as a result the value of the outlet temperature were computed. Finally, some analysis regarding the current closed Brayton cycle was carried out in order to evaluate the effect of the optical and thermal losses and other factors on its performance.

9.1 The Effect of Reflector's Size and Irradiance Value

In order to figure out how important is the amount of the received collected power and at the solar time, different parabolic dish diameter and irradiance values were deeply examined using 3D analysis. Generally speaking, the amount of incoming heat is strongly depends on the reflector diameter and the incoming irradiance at all the studied cases having said that, this was not the case regarding the optical efficiency of the thermal receiver. The main reason for that could be the losses of flux that occurs because of the shading losses which comes from the receiver shadow on the reflector which decreases the active area of the parabolic dish as shown in figure (6). By contrast the effect of both the diameter of parabolic dish reflector and the amount of irradiance on the incoming power, which reaches the parabolic dish reflector, is given in figure (7). From this figure it can be seen how this power is varying with respect to each; the irradiance value and the reflector diameter. So, in order to visualize the effect of the parabolic dish diameter, the latter was put as a parameter as shown in figure (8). This diagram presents how the overall optical efficiency of the system (thermal receiver and reflector) is increasing by increasing the reflector diameter, as a result of receiver shading- vade, until the value of 3.3 m when there was no increasing in the efficiency and this indicates that there is no point from making it larger than that.

9.2 The Effect of the Pitch Value

In this study the first step in the optical analysis is to find the optimum shape for each of the three receiver shapes. Hence, the optimums from the flux distribution view point when several attempts were carried on in order to find the configuration which can be covered by the reflected flux. So, some adjustments on each shape, to remove any length from the tube, which cannot be covered by the flux (dead areas), were carried out as shown in figure (9). The other important investigated factor is the effect of pitch values on each the optical and the thermal receiver functioning. Figure (10) shows the flux distribution for two different pitch values of the conical receiver shape which shows how

most of the flux will be directed to the cavity instead of the helical tube, which holds the working fluid. More analysis regarding the effect of this factor was carried out and the results have been showed in figures (11- 13). So, as shown in these figures, the amount of the absorbed heat by the cavity itself increased by increasing the pitch value which affects badly on the amount of absorbed flux by the helical tube. Even though the first figure, 10, presents the values at zero pitch, the amount of absorbed power by the cavity was in fact still high. This is because the analysed models were for the air domains for both the cavity and the helical tube; there is a small gap which represents the tube thickness. Beside the mentioned reason as well as the flux which hits the upper cover of the thermal receiver, there was an irradiance which has been absorbed by the cavity itself. The other two figures, 11 and 12, show how the absorbed power, by the cavity part, increased by increasing the pitch value from 0.25D to 0.5D.

9.3 The Thermal Analysis

Once the optical analysis completed, the real distribution of the three configurations of the thermal receiver with their model are exported to the Fluent solver in ANSYS® 17.2 in order to evaluate their performance from the thermal view point as well. Here, it is essential to highlight that all the optical and the thermal analysis have been achieved using 3-D analysis. So, as shown in figure (14) the real flux distribution was imported from the OptisWorks software to the fluent solver in ANSYS.

After reading each the coordinates and their amount of flux, using the UDF tool and choosing the correct setting and models, as previously mentioned in section 7, the software started and completed each run in about 15 hours. The results of each receiver configuration were firstly evaluated and the losses were highlighted and compared.

Figure (15) shows the comparison between the zero pitch and 0.5D pitch values in terms of both; the optical and thermal performances together for two models, with and without glass. From this figure it can be seen that the zero pitch was by far better than that of 0.5D value because of the lake of flux which hits the tube which initially results in decreasing the optical efficiency and as a result the overall receiver performance. Based on this result, only the zero pitch value models were considered for the other models in later analysis as shown in figure (16) for the spherical shape.

Figure (17) shows the amount of total heat losses for the three configurations of the studied thermal receiver at zero pitch values for both; with and without glass. From this figure it can be seen that the conical shape experienced the lowest values of total heat losses among the other glassed models with about 46, 45 and 56 Watt for the cylindrical, conical and spherical receiver shapes respectively. However, for the non-glassed models, these values were 64, 73 and 53 Watt in the same order with the shown percentage enhancement, in terms of the heat loss, of each receiver shape. The difference in the percentage enhancement values for the three shapes is, in fact, because of the difference in the internal volume for the three receiver shapes. That means the losses decrease with increasing the internal volume as a result of having lower heat inside the cavity which make the function of glass is

clearer i.e. at higher losses. Also, it can be seen that the conical shape experienced higher losses when there was no glass in its aperture which is unlike the results demonstrated in previous study, [14], and the reason for that is in that study the equality of the surface area values for the three receiver shapes was the based assumption.

Consequently, figure (18) presents the improvement, in terms of the receiver thermal efficiency, of each of the three configurations of the thermal receiver. From this figure it can be seen that an enhancement up to around 7% can be achieved by using the thermal glass as a cover for the aperture area where most of the heat losses is expected. Here it is important to emphasize that the difference in the amount of heat losses compared to the previous study [14] is because of the difference in the total surface area between the three receiver shapes. By contrast, in this study the emphasis was on having almost helical tube inside each receiver with almost no dead area with basically considering the same aperture area for the three receivers.

In order to evaluate the importance of considering the real flux by employing the UDF, which in fact a time consumer and need very long preparing to set each case study, instead of representing it as a uniformly distributed flux, the outlet temperature as being the most significant output factor for both (uniform and real distribution flux) was determined. Figure (19) shows the outlet temperature for the three receiver shapes at each; real and uniform flux (both were taken with glass covering the aperture area). Interestingly, it can be seen that there is insignificant difference between the total outlet air temperatures of the compressed air where the maximum difference was less than 2 K in the spherical shape. This indicates that it is accepted to assume a uniform flux on the helical surface tube with no considerable difference on the value of air flow exit temperature.

9.4 The Cycle Results

In order to figure out the performance of the studies solar powered closed Brayton cycle, a Matlab code has been initiated based on the series of equations mentioned in section 6. This has been achieved after evaluating the receiver optical and thermal performance and extracting the both losses, optical and thermal, from the power supplied to the system. The performance was evaluated based on four different outcomes; work done, heating power, thermal efficiency of the cycle and the overall system efficiency, which includes both cycle thermal efficiency and heating efficiency of the heating part of the system. As shown in figure (20) each; the heating power and the work output values were increasing by increasing both; the irradiance which is in fact not constant during days and seasons and the parabolic dish diameter. Furthermore the values of pressure ratio was the other factor which shows more influence on the work output of the cycle because of its direct relation between the net power output values. The overall indication on this figure is that the maximum work output and heating power which can be achieved from the studied system are 140 W and 600 W, 500 W and 2700 W and 1200 W and 5800 W for 1 m, 2 m and 3 m respectively.

Figure (21) shows both; the total efficiency, which shows more influence to the parabolic dish diameter, and the thermal efficiency against the pressure ratio at various irradiance values ranged from 500 W/m^2 to 1000 W/m^2 for three different parabolic dish diameter values, 1 m, 2 m and 3 m. From this figure it can be seen that the cycle thermal efficiency ranged from around 6% to 21% when the irradiance increased from 500 W/m^2 to 1000 W/m^2 and pressure ratio fluctuated from 1.1 to 6. Interestingly, this range of efficiency shows low influence to the dimeter of the parabolic dish reflector, because of the limited turbine inlet temperature as a result of increasing the mass flow rate. However, the opposite was the case for the overall system efficiency which was factored from about 64% to 80% by increasing the dish diameter from 1 m to 3 m.

10. Conclusions

Three dimensional simulation analysis using Matlab code and two other different tools (software) has been carried out in order to figure out the performance of three different configurations of small scale thermal receiver integrated in small scale solar powered closed Brayton cycle for domestic applications. The main out comes of the present studies can be concluded by the following bullets:

1- As the receiver shading effects badly on the amount of power which reach the parabolic dish reflector, there is an optimum diameter for the latter which can produce the highest optical efficiency for the all system.

2- Having the real flux, geometries and other boundary conditions are achievable by using the correct and relevant solver and settings however setting up this process is time consumer and compute-intensive.

3- Among the three investigated configurations of the thermal receiver, the conical one showed the best response when their aperture areas were covered by a specific thermal glass.

4- The conical receiver shape experienced the lowest amount of overall heat losses and the cylindrical was the worst one among them. Moreover, the thermal performance of the investigated zero pitch of the conical receiver is by far better than the 0.5D pitch value.

5- When the aperture area is covered by thermal glass, the outlet temperature of the compressed air showed insignificant influence to whether the distribution of flux, which hits the helical tube, is real or assuming to be constant. As a result the theory of assuming a constant (uniform) flux is valid.

6- More than one application, work and heat, can successfully be integrated in small scale solar powered closed Brayton cycle and an overall of 80% of the absorbed energy, by the receiver, can be achieved.

Nomenclature

A: Area (m^2)
Aa: Aperture area (m^2)
Cp: Specific heat (J/kg.K)
d: Diameter (m)
ε: Surface emissivity
F: View factor
g: Gravity (Kg)
Gr: Grashof number
h: Heat transfer coefficient
J: Radiosity
k: Thermal conductivity (W/m.K)
L: Characteristic length (m)
m: Mass flow rate of fluid
Nu: Nusselt number
Pr: Prandtl number
ρ: Density (Kg/m^3)
Q: Heat
θ : Inclination angle (Deg.)
Ra: Rayleigh number
u: Velocity component in x- direction (m/s)
T: Temperature (K)
μ: Viscosity (kg/m.s)
ϕ : Receiver inclination angle (Deg.)
x: Coordinate
ST: Energy source

Subscripts

1: Compressor inlet
2: Recuperator inlet of high pressure air
3: Receiver inlet
4: Turbine inlet
5: Recuperator inlet of low pressure air
6: Heat exchanger Inlet
Amb: Ambient
Ap: Aperture
Cav: Cavity
Cond: Conduction
Conv: Convection
i: Coordinate, inlet
f: Fluid
o: Outlet
Rad: Radiation
Ref: Reflector
Rec: Receiver
Sur: Surface area
T: Total
W: Wall or cavity internal surface
WI: With insulation

Abbreviation

abs: Absorbed heat
C: Compressor
CR: Cavity Receiver
G: Generator
H: Heat Exchanger
In: Total incoming power from the sun
P: Pump
PD: Parabolic Dish
R: Recuperator
Sys: System
Th: Thermal
T: Turbine

WST: Water Storage Tank

ACKNOWLEDGMENT

The author thanks the Higher Committee of Developing Education in Iraq HCED for funding this project.

References

[1] LD Jaffe. Dish concentrators for solar thermal energy. J Energy 7(4) (1981), pp304-312.
[2] W.G. Le Roux, Solar tracking for a parabolic dish used in a solar thermal Brayton cycle.
[3] Tu, Nan, Jinjia Wei, and Jiabin Fang. "Numerical study on thermal performance of a solar cavity receiver with different depths." Applied Thermal Engineering 72.1 (2014): 20-28.
[4] Li, Zhigang, et al. "Study on the radiation flux and temperature distributions of the concentrator–receiver system in a solar dish/Stirling power facility." Applied Thermal Engineering 31.10 (2011): 1780-1789.
[5] Loni, R., et al. "Performance study of a solar-assisted organic Rankine cycle using a dish-mounted rectangular-cavity tubular solar receiver." Applied Thermal Engineering 108 (2016): 1298-1309.
[6] Daabo, Ahmed M., Saad Mahmoud, and Raya K. Al-Dadah. "The effect of receiver geometry on the optical performance of a small-scale solar cavity receiver for parabolic dish applications." Energy 114 (2016): 513-525.
[7] Daabo, Ahmed, Saad Mahmoud, and AL-Dadah Raya. "Effect of open cavity configuration on solar receiver thermal performance." Extended Abstracts. 2016.
[8] Patil, Milind, Ramchandra Jahagirdar, and Eknath Deore. "Experimental investigation of heat loss from hemispherical solar concentrator receiver." Frontiers in Heat and Mass Transfer (FHMT) 3.3 (2012).
[9] Wu, Shuang-Ying, et al. "Experimental Study on The Effect of Wind on Heat Losses from a Fully Open Cylindrical Cavity with only Bottom Wall Heated." International Journal of Green Energy 12.12 (2015): 1244-1254.
[10] Paitoonsurikarn, S., and K. Lovegrove. "Numerical investigation of natural convection loss in cavity-type solar receivers." Proceedings of Solar. 2002.
[11] Harris, James A., and Terry G. Lenz. "Thermal performance of solar concentrator/cavity receiver systems." Solar energy 34.2 (1985): 135-142.
[12] T. Taumoefolau and K. Lovegrove. An experimental study of natural convection heat loss from a solar concentrator cavity receiver at varying orientation. Australia, 2002.
[13] Reddy, K. S., and N. Sendhil Kumar. "Combined laminar natural convection and surface radiation heat transfer in a modified cavity receiver of solar parabolic dish." International Journal of Thermal Sciences 47.12 (2008): 1647-1657.
[14] Daabo, Ahmed M., Saad Mahmoud, and Raya K. Al-Dadah. "The optical efficiency of three different geometries of a small scale cavity receiver for concentrated solar applications." Applied Energy 179 (2016): 1081-1096.
[15] Loni, R., et al. "Optimizing the efficiency of a solar receiver with tubular cylindrical cavity for a solar-powered organic Rankine cycle." Energy 112 (2016): 1259-1272.
[16] Wei, Min, et al. "Fluid flow distribution optimization for minimizing the peak temperature of a tubular solar receiver." Energy 91 (2015): 663-677.
[17] Boyaghchi, Fateme Ahmadi, Mansoure Chavoshi, and Vajiheh Sabeti. "Optimization of a novel combined cooling, heating and power cycle driven by geothermal and solar energies using the water/CuO (copper oxide) nanofluid." Energy 91 (2015): 685-699.
[18] Daabo, Ahmed M., et al. "Numerical investigation of pitch value on thermal performance of solar receiver for solar powered Brayton cycle application." Energy 119 (2017): 523-539.
[19] Zhirong Liao, Xin Li, Chao Xu, Chun Chang and Zhifeng Wang. Allowable flux density on a solar central receiver. Renewable Energy 62 (2014) 747e753, China, 2013.
[20] Prakash, M. "Numerical Study of Natural Convection Heat Loss from Cylindrical Solar Cavity Receivers." ISRN Renewable Energy 2014 (2014).

[21] Wang, Mo, and Kamran Siddiqui. "The impact of geometrical parameters on the thermal performance of a solar receiver of dish-type concentrated solar energy system." Renewable Energy 35.11 (2010): 2501-2513.
[22] Bergman, Theodore L., Frank P. Incropera, and Adrienne S. Lavine. Fundamentals of heat and mass transfer. John Wiley & Sons, 2011.
[23] A. Bejan, Heat Transfer, John Wiley & Sons, 1993.
[24] Paitoonsurikarn, S., and K. Lovegrove. "On the study of convection loss from open cavity receivers in solar paraboloidal dish applications" Proceedings of Solar. 2003.
[25] M. Prakash. Numerical study of natural convection heat loss from cylindrical solar cavity receiver. Hindawi Publishing Corporation. Article ID 104686, Volume 2014. India, 2014.
[26] Kumar, N. Sendhil, and K. S. Reddy. "Numerical investigation of natural convection heat loss in modified cavity receiver for fuzzy focal solar dish concentrator." Solar Energy 81.7 (2007): 846-855.
[27] Holman J.P. (1997) Heat transfer, 8th edition, New York: McGraw-Hill Companies.
[28] Jilte, R. D., S. B. Kedare, and J. K. Nayak. "Natural convection and radiation heat loss from open cavities of different shapes and sizes used with dish concentrator." Mechanical Engineering Research 3.1 (2013): 25.
[29] Wu, Y. C., and L. C. Wen. "Solar receiver performance of point focusing collector system." American Society of Mechanical Engineers 1 (1978).
[30] Sellami, Nazmi, and Tapas K. Mallick. "Optical efficiency study of PV crossed compound parabolic concentrator." Applied Energy 102 (2013): 868-876.
[31] Al-Shohani, Wisam AM, et al. "Optimum design of V-trough concentrator for photovoltaic applications." Solar Energy 140 (2016): 241-254.
[32] Al- Gareu, Abdulmaged, et al. "357: Optical analysis of flux uniformity and efficiency in low concentrating PV systems." SUSTAINABLE ENERGY: 811.
[33] Sellami, Nazmi, and Tapas K. Mallick. "Optical characterisation and optimisation of a static Window Integrated Concentrating Photovoltaic system." Solar Energy 91 (2013): 273-282.
[34] Ali, Imhamed M. Saleh, et al. "An optical analysis of a static 3-D solar concentrator." Solar Energy 88 (2013): 57-70.
[35] Yuan, James K., Clifford K. Ho, and Joshua M. Christian. "Numerical Simulation of Natural Convection in Solar Cavity Receivers." Journal of Solar Energy Engineering 137.3 (2015): 031004.
[36] Versteeg, Henk Kaarle, and Weeratunge Malalasekera. An introduction to computational fluid dynamics: the finite volume method. Pearson Education, 2007.
[37] "Ansys fluent theory guide." http://www.ansys.com, 2015.
[38] Daabo, Ahmed M., Saad Mahmoud, and Raya K. Al-Dadah. "Development of Small-Scale Axial Turbine for solar powered Brayton Cycle." Students on Applied Engineering (ISCAE), International Conference for. IEEE, 2016.
[39] Kumar, N. Sendhil, and K. S. Reddy. "Numerical investigation of natural convection heat loss in modified cavity receiver for fuzzy focal solar dish concentrator." Solar Energy 81.7 (2007): 846-855.
[40] Ngo, L. C., Tunde Bello-Ochende, and Josua P. Meyer. "Three-dimensional analysis and numerical optimization of combined natural convection and radiation heat loss in solar cavity receiver with plate fins insert." Energy Conversion and Management 101 (2015): 757-766.
[41] ANSYS 15 CFX-Solver Theory Guide.
[42] Abdullahi, B., et al. "Optical and thermal performance of double receiver compound parabolic concentrator." Applied Energy 159 (2015): 1-10.
[43] Clausing, A. M. "An analysis of convective losses from cavity solar central receivers." Solar Energy 27.4 (1981): 295-300.
[44] Stine, William B., and C. G. McDonald. "Cavity receiver convective heat loss." International Solar Energy Society, Solar World Congress (1989, Kobe, Japon). 1989.
[45] Taumoefolau, T., et al. "Experimental investigation of natural convection heat loss from a model solar concentrator cavity receiver." Journal of Solar Energy Engineering 126.2 (2004): 801-807.

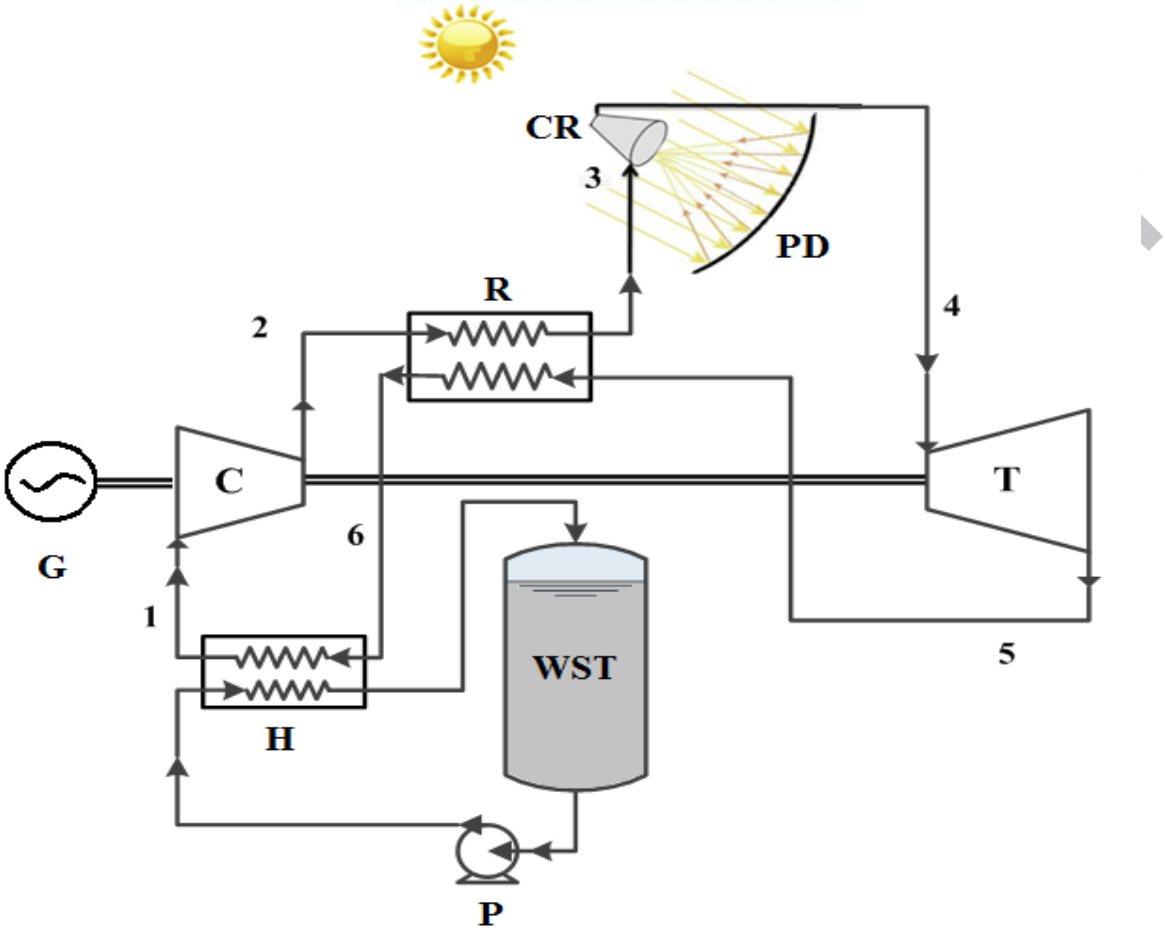

Fig.1: Schematic diagram of the small scale solar powered closed Brayton cycle.

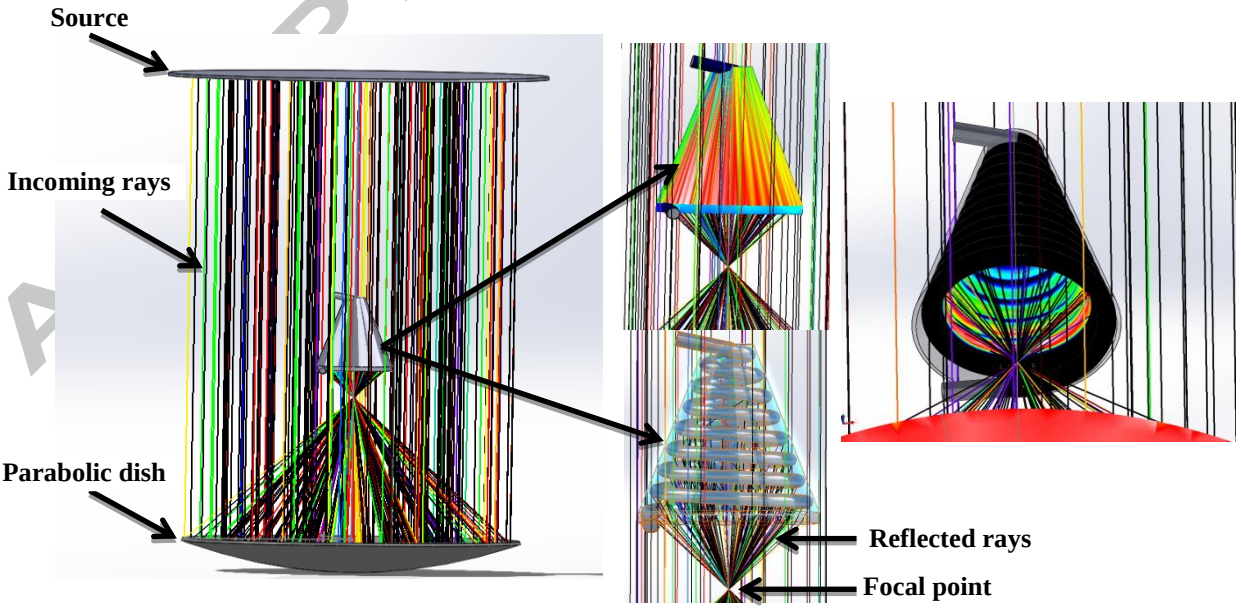

Fig.2: The parabolic dish reflector together with the modelled conical shape receiver, all through the ray-tracing analysis using OptisWorks.

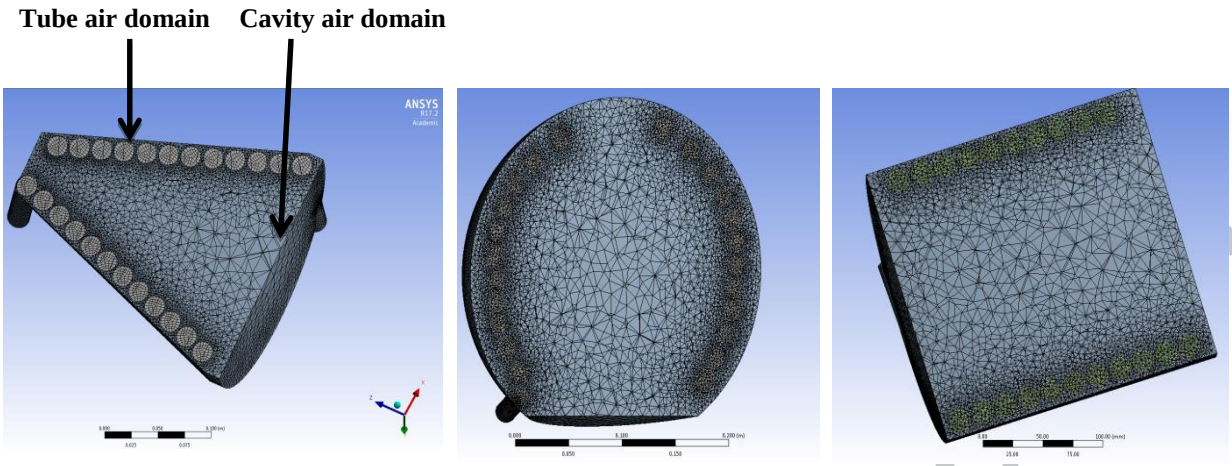

Fig.3A: The meshed shape of the air domains for both the cavity receiver and its helical tube modelled in ANSYS® 17.2.

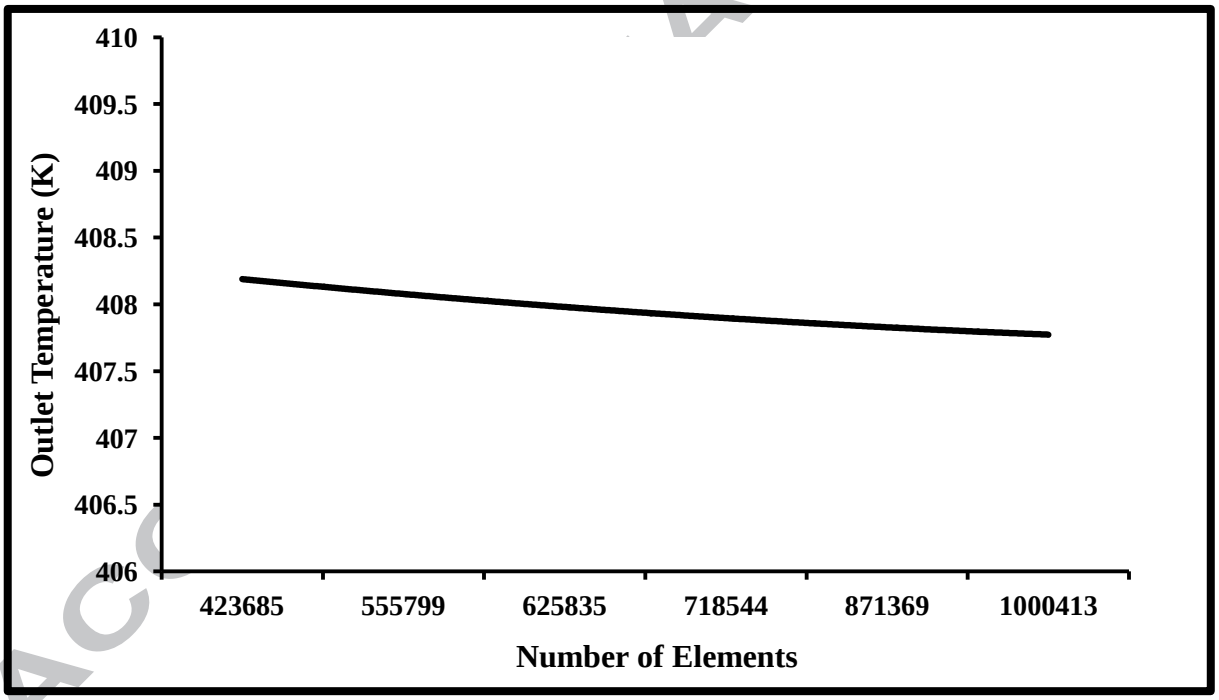

Fig.3B: Mesh sensitivity based on the receiver outlet temperature.

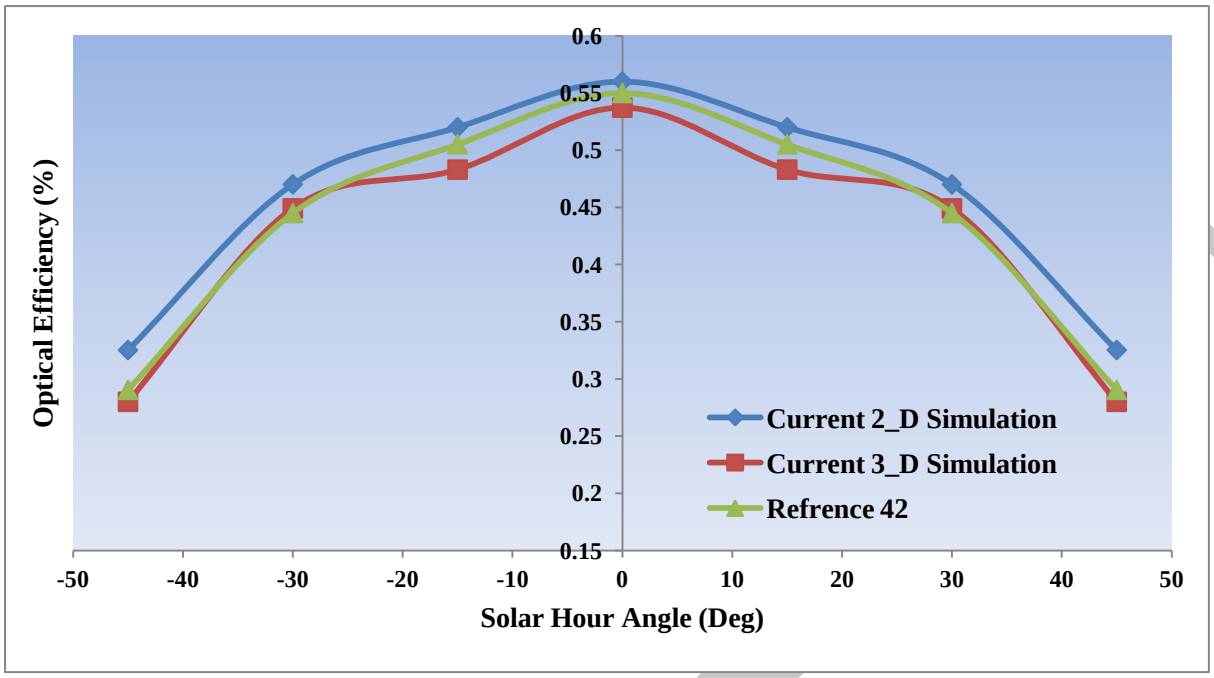

Fig. 4: The optical validation achieved against a previous study mentioned in reference [42].

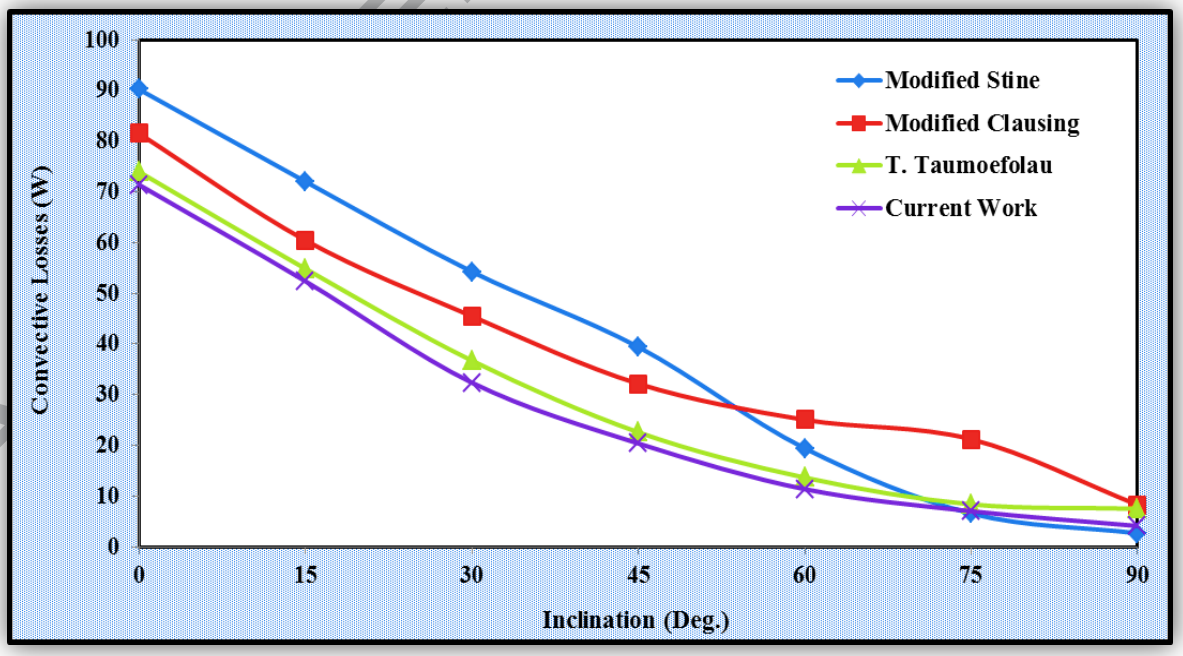

Fig. 5: Comparison of the amount of receiver convective losses between the current study and three other experimental studies found in literature.

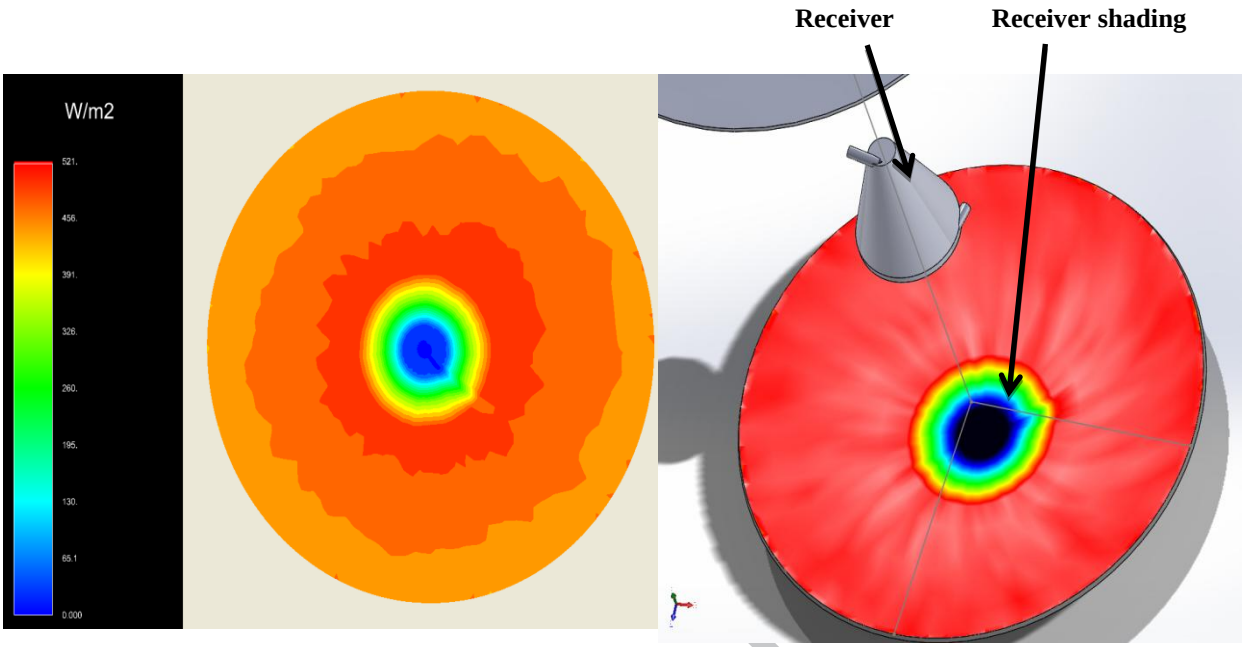

Fig. 6: The effect of receiver body shading on the received flux from the source for 1 m diameter parabolic dish reflector (Optically using OptisWorks).

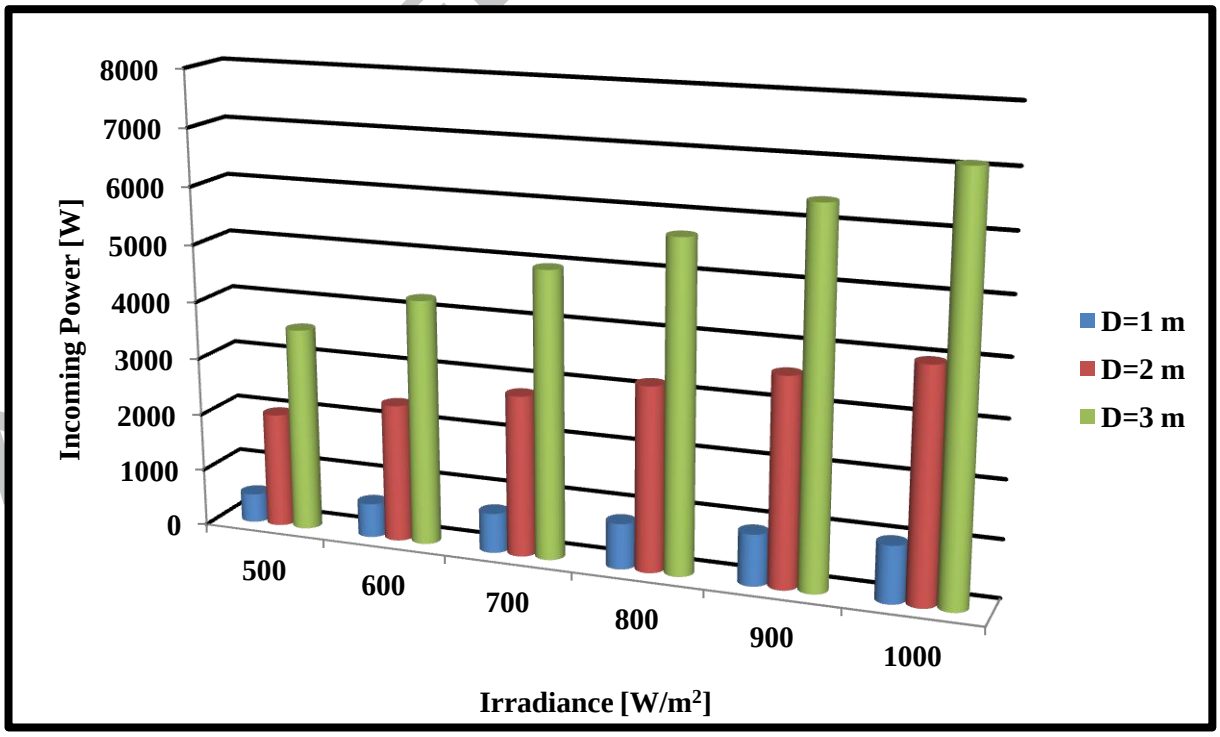

Fig. 7: Total incoming power from the sun at various irradiance and parabolic dish diameter values.

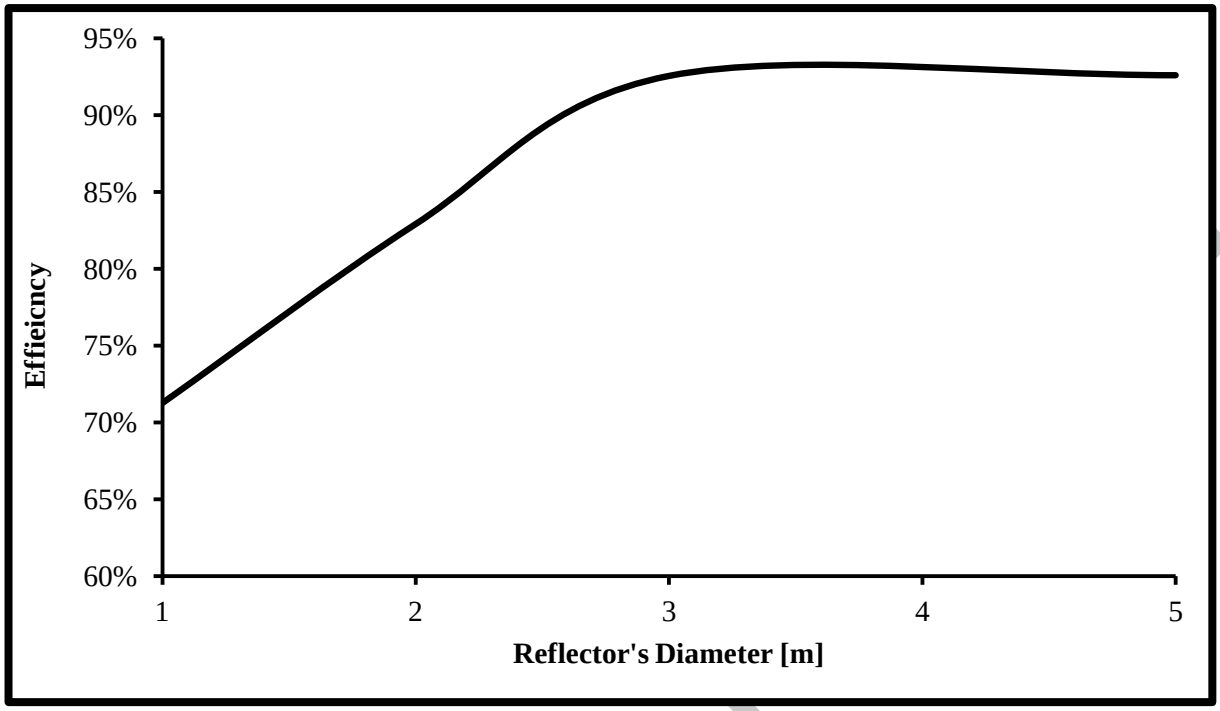

Fig. 8: The optimum performance of the designed parabolic dish reflector, in terms of the optical efficiency, at different diameter values.

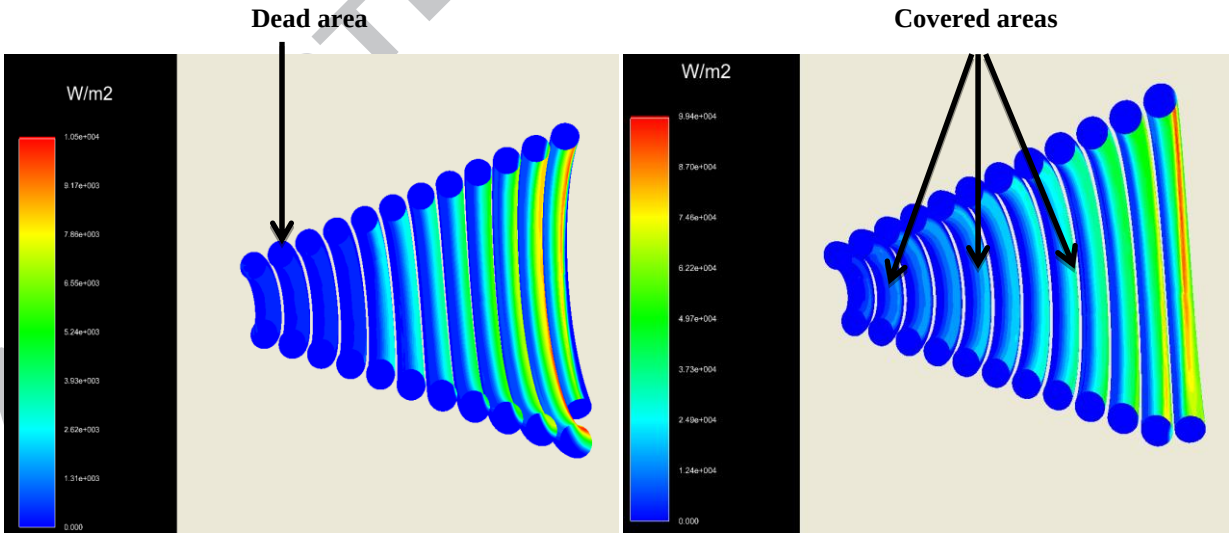

Fig. 9: Absorbed power by each; the helical tube of the conical receiver cavity at two different configurations; (left): With some dead areas and (right) most of the tube surface area was covered by the flux (Optically using OptisWorks).

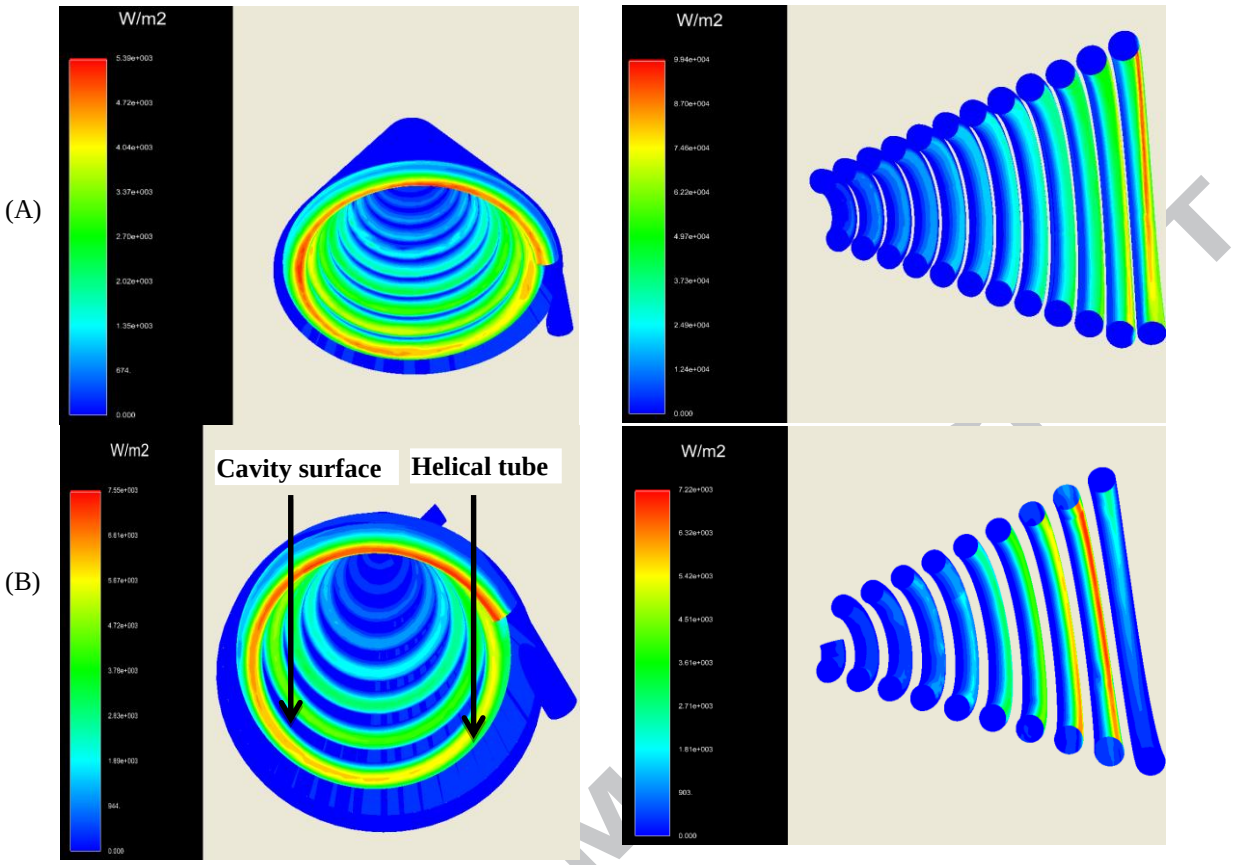

Fig. 10: Absorbed power by each; the receiver cavity and its helical tube at two different pitch values; (A): Zero pitch and (B) 0.5D pitch (Optically using OptisWorks).

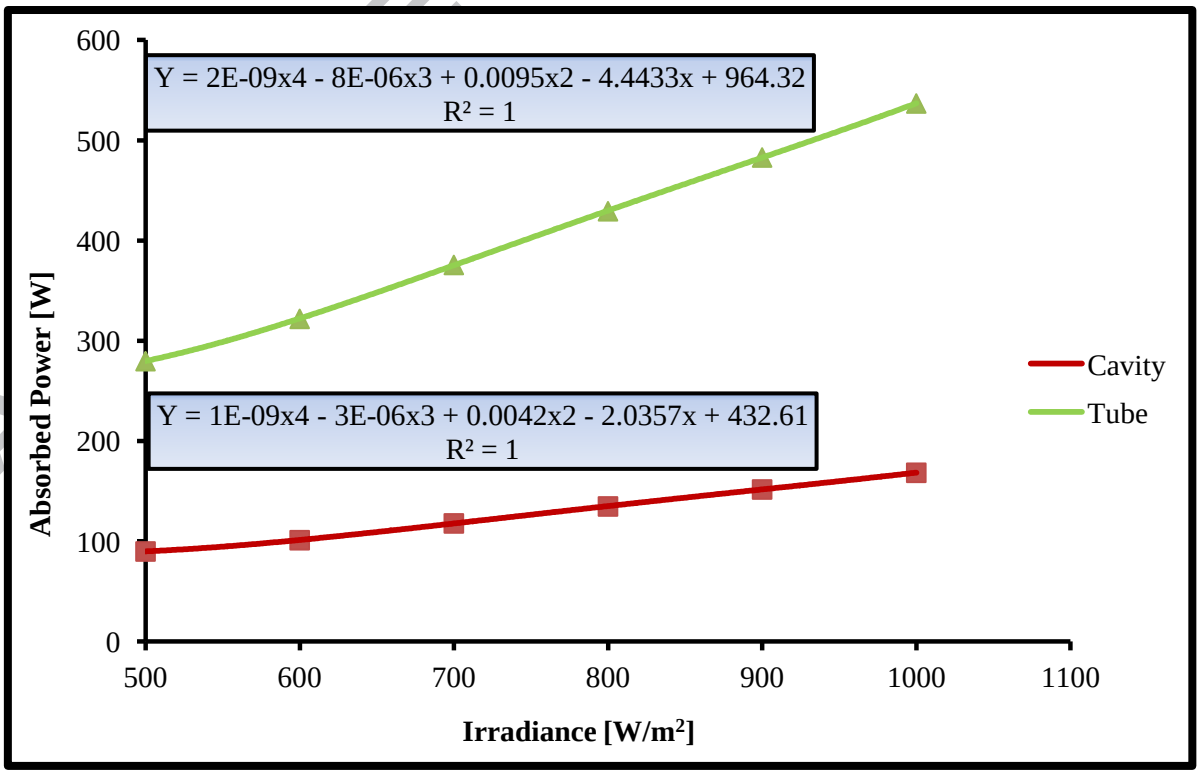

Fig. 11: Absorbed power by each; the conical receiver cavity and its helical tube at zero pitch and different irradiance values (Optically).

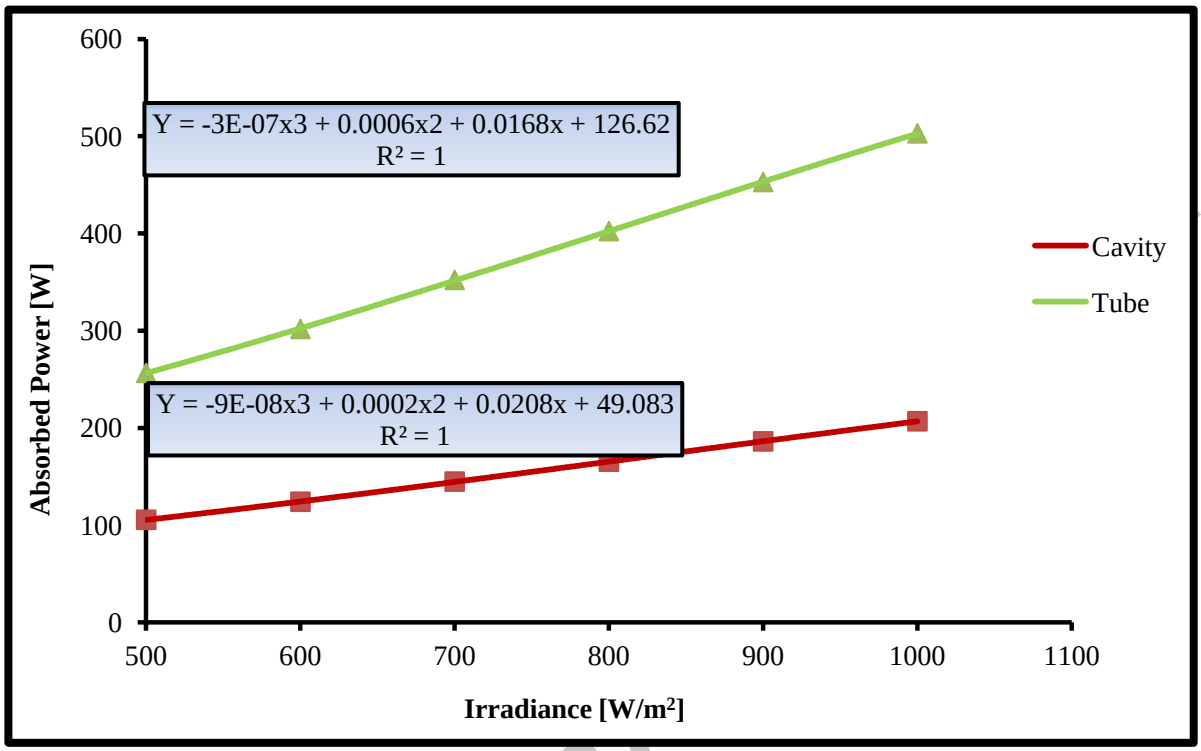

Fig. 12: Absorbed power by each; the cylindrical receiver cavity and its helical tube at 0.25D pitch value and different irradiance values (Optically).

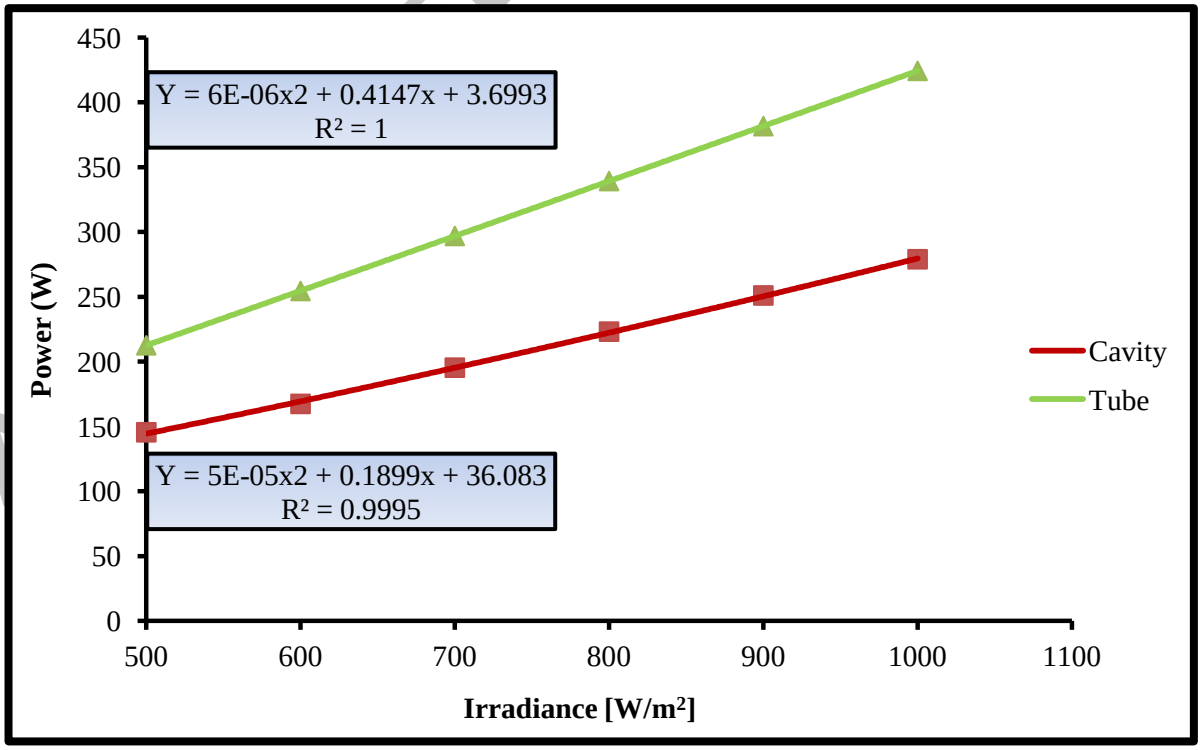

Fig. 13: Absorbed power by each; the spherical receiver cavity and its helical tube at 0.5D pitch value and different irradiance values (Optically).

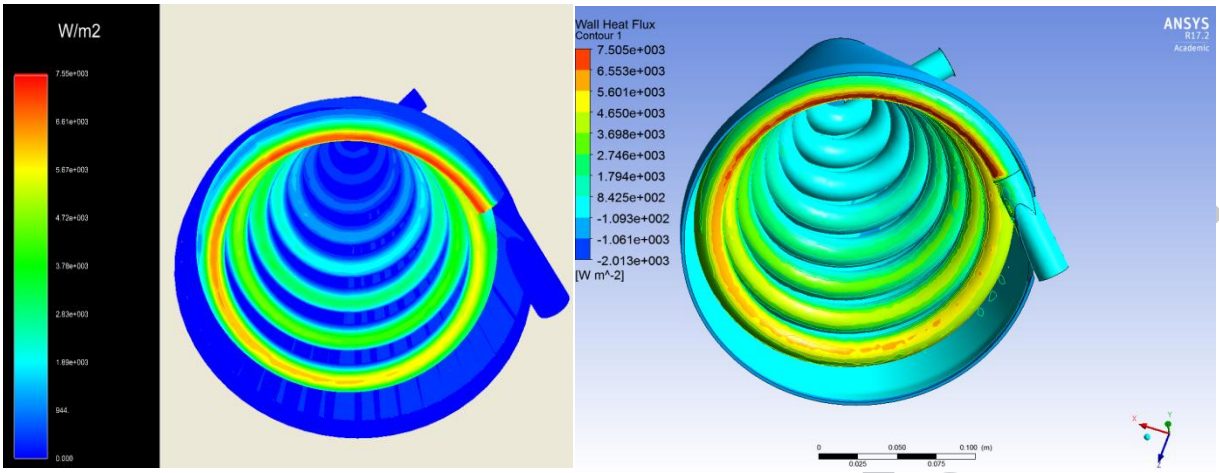

Fig. 14: Flux distribution in 3-D for the conical shape receiver at 0.5D pitch in OptisWorks, left, and the imported flux to the ANSYS fluent, on the right.

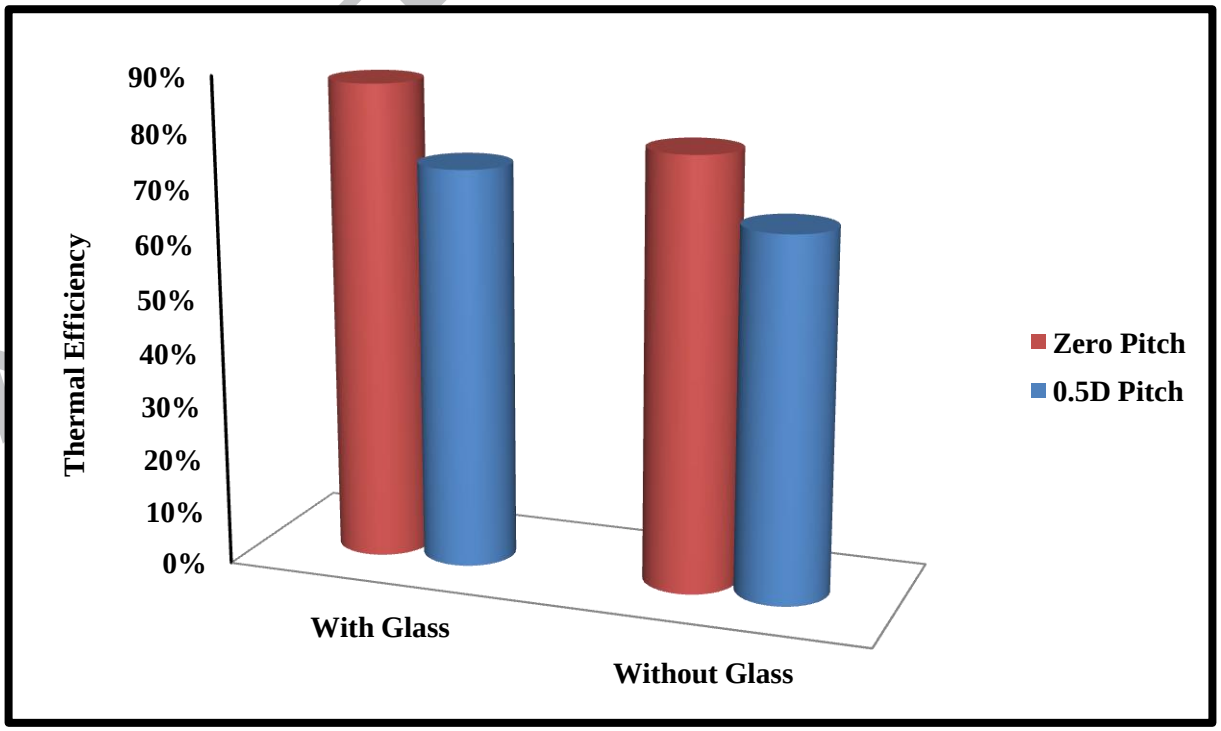

Fig. 15: The thermal efficiency at two different pitch values of the conical shape with and without glass.

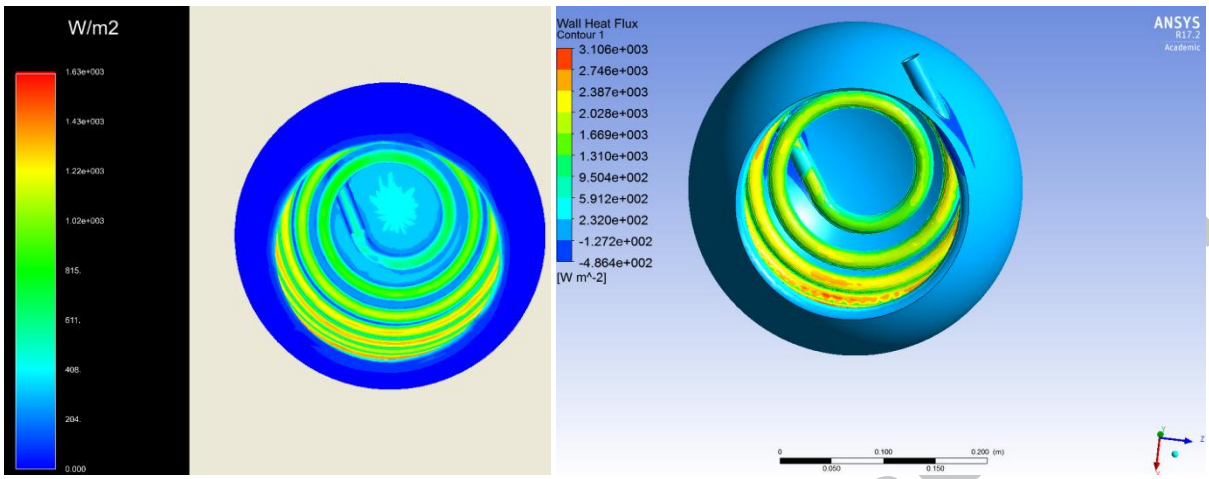

Fig. 16: Flux distribution in 3-D for the spherical shape receiver at zero pitch in OptisWorks, left, and the imported profile of flux in ANSYS fluent, on the right.

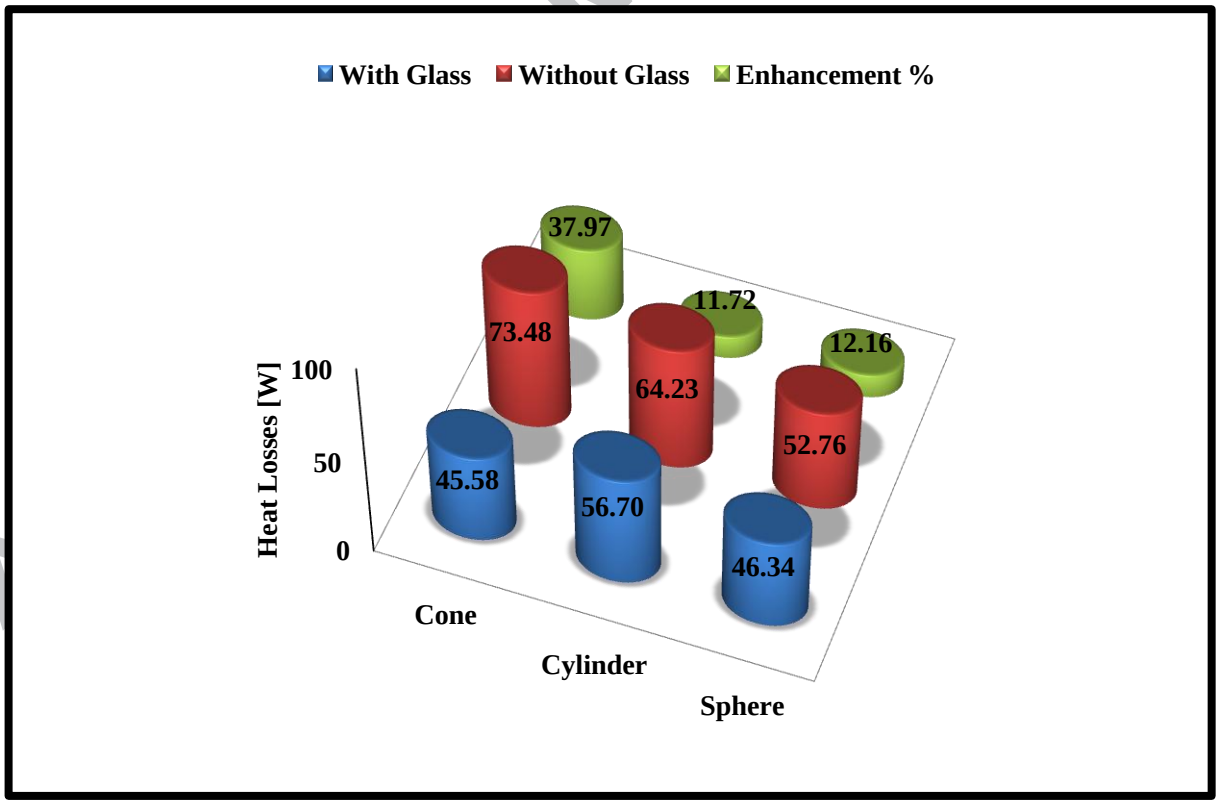

Fig. 17: Total heat losses for the three configurations at zero pitch with and without glass.

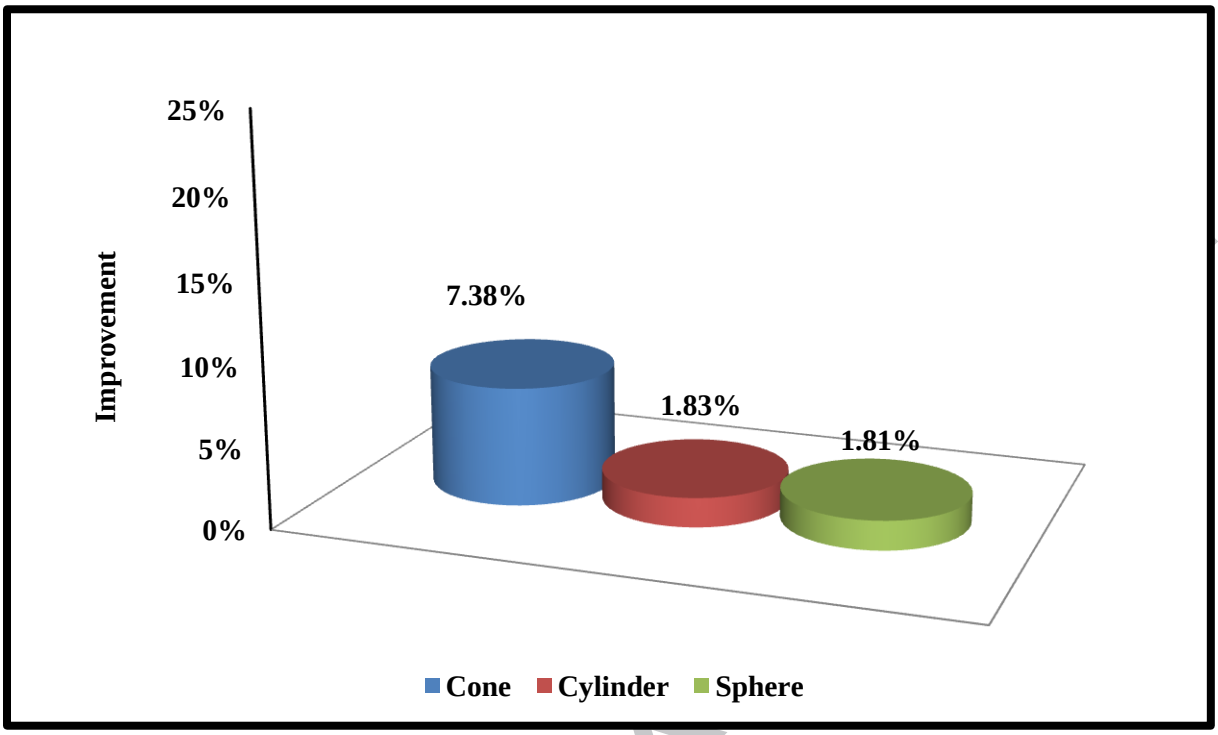

Fig. 18: The percentage improvement in the thermal performance for the three configurations because adding glass.

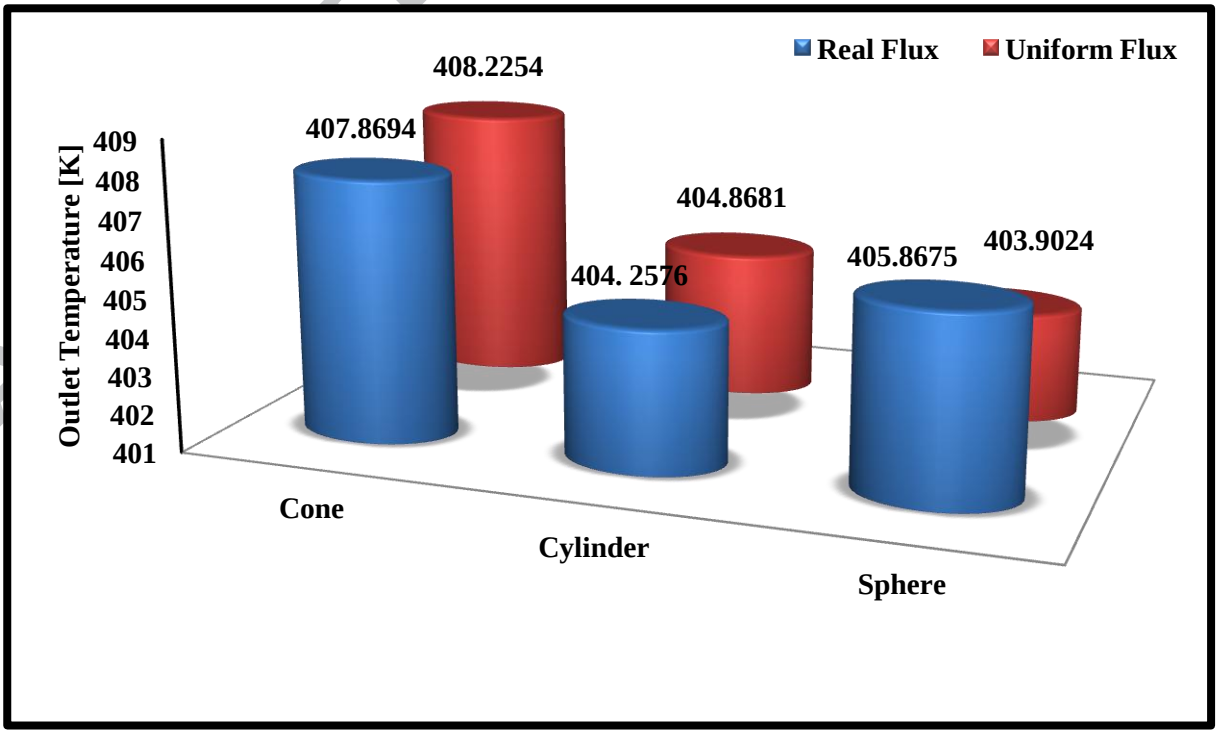

Fig. 19: Total air outlet temperature for the three shapes at uniform and real flux modelling.

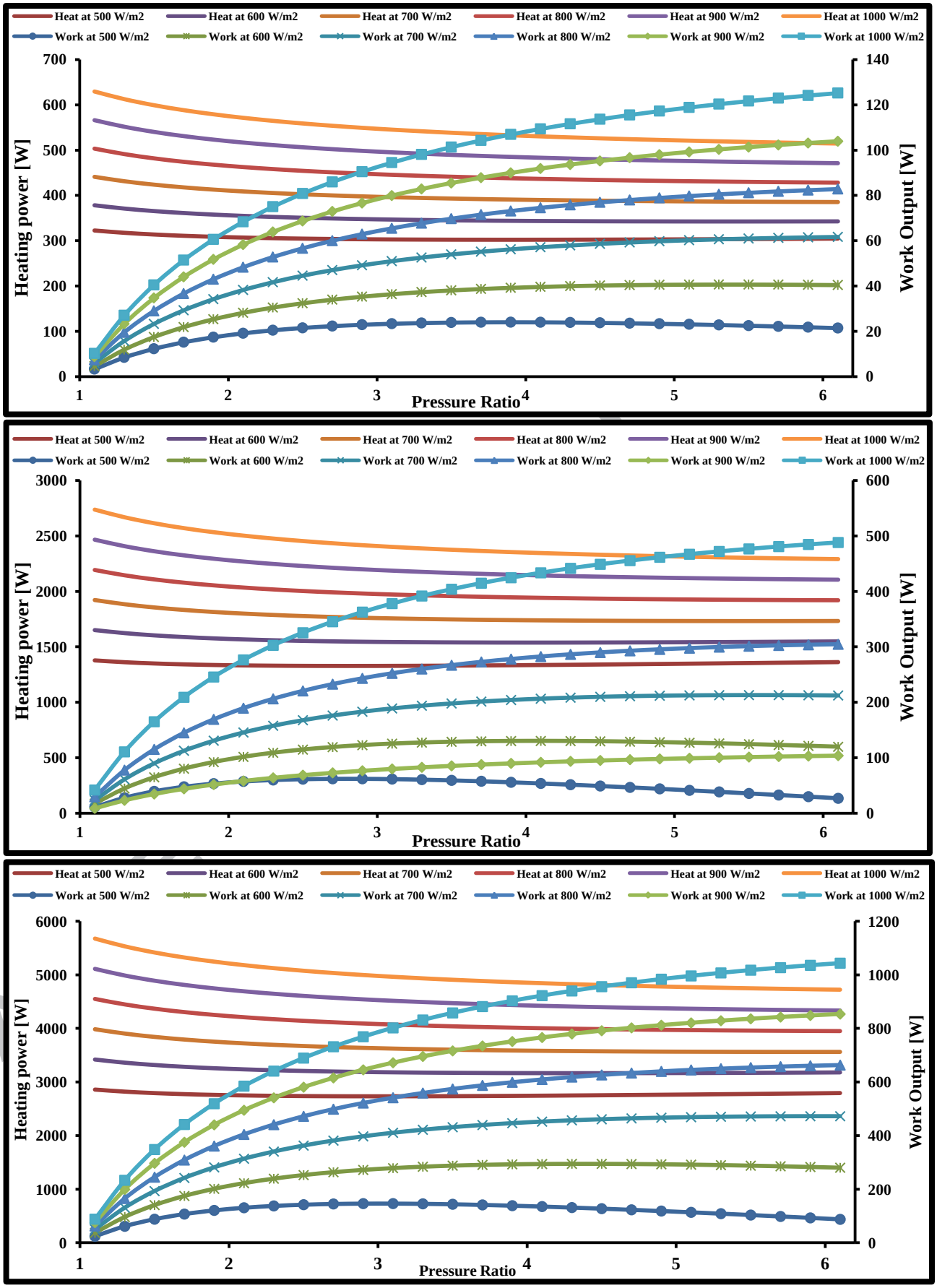

Fig. 20: Work output and heating power at various irradiance values and three parabolic dish dimeters values; 1 m, 2 m and 3 m for the upper, middle and lower figures respectively.

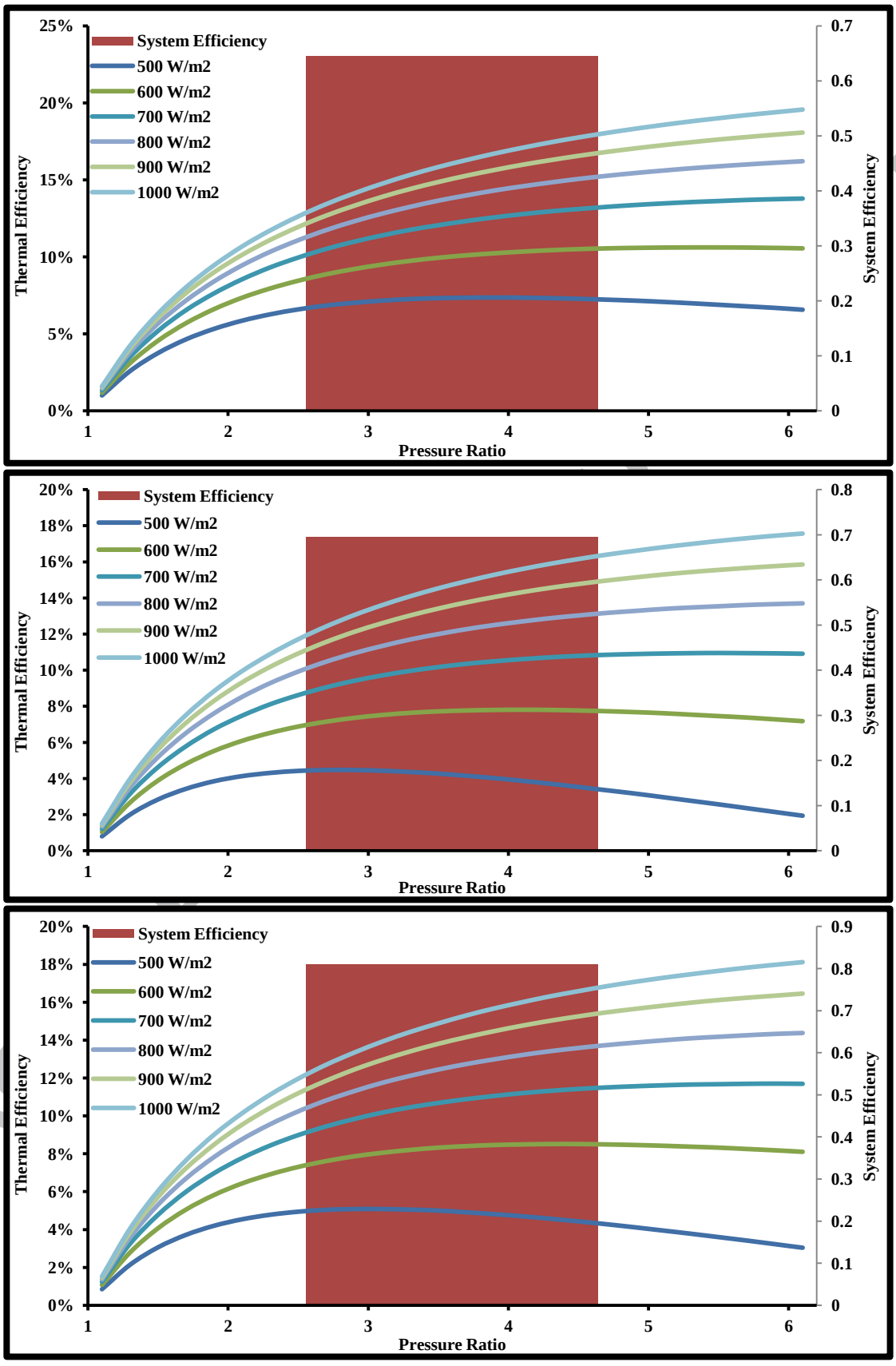

Fig. 21: Thermal and overall system efficiency values of the cycle at various values of both irradiance and pressure ratio and three parabolic dish diameter values; 1 m, 2 m and 3 m for the upper, middle and lower figures respectively.

Table I: Dimensions of the Analysed Components (Parabolic Dish and Thermal Cavity Receivers)

Component	Aperture Diameter (m)	Height (m)	Inclination (Deg.)	Thickness (m)
Parabolic Dish	1, 2,3,4 and 5	-	45^{o} (Tilt angle)	0.01
Conical Shape	0.225	0.24	19^{o}	0.03
Cylindrical Shape	0.225	0.235	0	0.03
Spherical Shape	0.225	0.257	270^{o}	0.03

Table II: Dimensions of the Helical Tube Used Inside the Three Receiver Shapes.

Component	Diameter (m)	Length (m)	Internal Diameter(m)	Thickness (m)
Helical Conical	0.2	4.3724	0.019	0.001
Helical Cylindrical	0.2	6.6006	0.019	0.001
Helical Spherical	0.2	8.534	0.019	0.001

Table III: Properties of the Used Material in the Thermal Analysis.

Material	Density (kg/m^3)	Cp Specific Heat (J/kg.K)	Thermal Conductivity (W/m.K)
Glass	2500	840	1
Copper	8978	381	387.6
Insulation Material	50	800	0.09

Highlights

- **The performance of small scale solar powered closed Brayton cycle has been proposed.**
- **The optimum shape of each receiver configuration has been, optically, achieved.**
- **The real flux distribution on the helical tube surface inside each receiver has been used.**
- **An enhancement in the thermal performance of studied cavity receivers has been achieved.**